journal
OF THE INSTITUTE OF ENERGY
JUNE 1997

CONTENTS

the institute of energy

Journal of the
Institute of Energy

Vol LXX No 483 June 1997

Contents

Published quarterly from the headquarters of The Institute of Energy
18 Devonshire Street, London W1N 2AU

Telephone: 0171-580 7124 (Administration and Accounts)
0171-580 0008 (Conferences)
0171-580 0077 (Membership, Education and Journal Subscriptions)
Fax: 0171-580 4420

Subscription rate £130.00 post free (4 issues).
Single copies of the *Journal of The Institute of Energy:* £40.00 (post free).

Journal of the Institute of Energy, June 1997, 70, pp 57-70

Predictions of particulate formation, oxidation and distribution in a three-dimensional oil-fired furnace

J YUAN, V SEMIÃO and M G CARVALHO*

The prediction of a three-dimensional oil-fired industrial-type furnace is described. The gas-phase combustion-related properties are calculated by means of time-averaged Eulerian conservation equations, in addition to the k-ε turbulence model. The droplets and cenospheres balance equations are solved in Lagrangian fashion, with a stochastic approach for turbulent dispersion. The different phases are coupled through mass, momentum and energy exchange processes, assuming negligible influence of local discontinuities induced by the non-gaseous phase. The turbulent-diffusion flame is modelled by means of a clipped-Gaussian pdf to account for fluctuations of scalar properties. Chemistry is assumed to be fast. Radiation is modelled by the discrete transfer method. Oil combustion particulate, namely soot formed during gas-phase reactions, and cenospheres formed by the liquid-phase pyrolysis, may contribute to fouling, heat-transfer and emissions. Soot was modelled by solution of its Eulerian transport equation. In this work a Lagrangian model to predict formation, oxidation and spatial distribution of cenospheres is used. Soot is found to form in the fuel-rich edges of the flame; because of its fast oxidation, it contributes significantly to radiation only. On the other hand cenospheres, because of their structure and size, contribute significantly to fouling and emissions.

1 Nomenclature

A	constant of soot oxidation rate
A_c	constant of coke-particle oxidation rate
$a_{m,n,n'}$	constants for calculating ε_m
c	soot concentration, kg m^{-3}
C_D	drag coefficient
C_f	constant of soot-formation rate
CFI	coke formation index
$C_{p,i}$	specific heat of species i
D_i	diameter of i-disperse phase
D_{O_2}	binary mass diffusion coefficient of O_2 in Eqn (17)
E	activation energy of Arrhenius terms
g	gravity constant
K_g	thermal conductivity of gas
k	turbulent kinetic energy
$k_{g,n}$ $k_{s,n'}$	constants for calculating ε_m
L	latent heat of vaporisation; path length in Eqn (1)
Nu	Nusselt Number
n	constant of soot-formation model
m_i	mass fraction of species i
Pr	Prandtl Number
p_i	partial pressure of species i
R	universal gas constant
Re	Reynolds Number
S_d	soot oxidation rate
S_f	soot formation rate
s_i	stoichiometric oxygen requirement for oxidation of species i
T	temperature, K
u	velocity component in the x direction
v	velocity component in the y direction
w	velocity component in the z direction
$\bar{v}$	velocity vector
ε	dissipation rate of turbulent kinetic energy
ε_m	total emittance of gas-soot mixture
μ	absolute viscosity
ρ	density
τ	thickness of the coke particle shell in Eqn (15)
τ_d	characteristic response time of droplet
ϕ	equivalence ratio

Subscripts

c	carbon dioxide (partial pressure subscript); coke particle
d	droplet
f	fuel
g	gas
o	oxygen
s	soot
w	water vapour

1 Introduction

1.1 Preamble

Combustion and pollution have been virtually inseparable since mankind's discovery of fire. As a result of concerted, world-wide concern during the past two decades, regarding emissions from factory smokestacks and vehicle tailpipes, great strides have been made towards the clean combustion of fuels. The steadily increasing severity of emission regulations has led to much research into the mechanisms of pollutant formation. In addition, limited energy resources and rising fuel prices promoted considerable interest from intensive users of industrial energy, in supporting the creation of mathematical models that reliably simulate the performance of combustors.

Traditionally, the design of combustors has been based on the use of empirical models that attempt to correlate overall performance in terms of simple global parameters such as combustor volume, inlet air temperature and pressure,

*J Yuan, Visiting Professor; V Semião, Assistant Professor and corresponding author; and M G Carvalho, Full Professor; Departamento de Engenharia Mecânica, Instituto Superior Técnico, Av Rovisco Pais, 1096 Lisboa Codex, Portugal.

mass flow rate and fuel:air ratio. However, a more fundamental approach is required both by the need for energy savings and by the necessity to reduce the emission of pollutants from such systems. In fact, increasing pressure has been placed on engineers to develop theoretical and experimental methods that are able to quantify and enhance the performance of industrial combustors. Particularly acute is the need to comply with more stringent ecological requirements, by lowering noxious emissions without sacrificing production.

On oxidation, ideally the combustion process would convert all the sulphur to SO_2, the nitrogen to NO, the hydrogen to water vapour and the carbon to CO_2. Combustion is not ideal, however, and analysis of combustion products reveals the presence of products such as SO_2, SO_3, NO, NO_2, CO, CO_2, H_2O, H_2, unburnt hydrocarbons, polycyclic aromatic hydrocarbons and particulate. Most of these are pollutants.

Fouling within industrial furnaces is a relatively recent research subject, because of its noxious nature and its interference in the combustion process. In oil-fired combustion chambers fouling can interact with the efficiency of the process, as the sets of deposition mechanisms that are active in high-temperature regimes can significantly affect heat-transfer processes. Indeed, particulates formed during oil combustion produce deposits on the walls, which reduce heat-transfer and thereby influence combustion reactions. Prediction codes exist that are capable of computing the aerodynamics, mixing, combustion and thermal radiation in industrial combustors to a reasonable degree of accuracy. However, these predictive tools have been far from adequately employed as a means of permitting the knowledge of particulate distribution inside furnaces, and emissions reduction control, to be applied directly in the quest for improved burner and combustor designs.

The control of fouling inside combustion chambers is probably achievable through combustion modifications, and to some extent through optimisation of operating conditions; but parametric trials on full-scale equipment are very expensive, and accurate measurements are difficult. The number, and hence the cost, of trials required to be performed could be reduced considerably with the aid of reliable mathematical modelling.

The present paper describes the application of full three-dimensional mathematical modelling to an industrial-type furnace. The turbulence, combustion and radiation physical models are those used previously by the authors to determine the emissions of nitric oxide from a cross-fired regenerative glass furnace[1]. In the present work the two-dimensional models for particulate formation and oxidation, developed by the authors and validated against experimental data acquired in an axially symmetric geometry[2], were extended to three-dimensional modelling. They were then applied to an industrial-type furnace for evaluation of their effect on fouling, heat-transfer and emissions to the atmosphere.

1.2 Particulate formation and oxidation mechanisms

According to the phase where particulate precursor reactions occur, oil combustion can lead to the formation of solid particles of two distinct kinds. Soot is formed during gas-phase reactions, and usually exhibits sizes smaller than one micrometre. Conversely, coke particles are the result of the liquid-phase pyrolysis of the heavy fuel-oil droplets, and are larger. (Typical values[3] of coke particle sizes are within the range of 1 to 50 μm, and sometimes[4] even with a few hundred micrometres.) These coke particles have a porous structure, each one comprising a carbonaceous shell containing several blowholes, and it is within these hard cenospheres that fuel impurities concentrate. Many investigators have studied the formation and oxidation of soot and cenospheres in oil combustion[3-9]. The previous works have shown that particulate formation and oxidation, in addition to varying with the fuel properties, depend on the temperature and oxygen levels surrounding the droplet.

To a great extent the effects on fouling, heat-transfer and emissions are determined by particulate formation and oxidation processes, and by its spatial distribution inside the furnace. Therefore the correct quantification of the above-mentioned physical processes requires the knowledge of the spatial distribution of particulate within oil-fired combustion chambers. As regards soot, very little of the fuel-carbon appears in this form, so the primary function of the soot model is the good characterisation of the optical properties of the flame. Some models for its formation and oxidation rates have been developed and coupled with numerical codes for simulation of oil combustion[8]. One of those models was selected and embedded in the numerical algorithm presented herein, together with the mathematical modelling of flow, combustion and heat-transfer.

The physical mechanisms for the formation and oxidation of coke particles have also been experimentally studied[3,4,6,7,9]. However, these experimental results are far from being extensively used and applied to numerical modelling of industrial furnaces. Moreover, to the knowledge of the authors no previous works have reported three-dimensional numerical predictions in oil-fired furnaces for both soot and coke particulate. In this work, besides the above-mentioned soot modelling, physical models for coke particulate formation and oxidation are used. These models are based on the experimental results of Urban *et al*[6,9] and were extended from the two-dimensional validated predictions[2] to three-dimensional modelling, in order to be coupled with the Lagrangian approach used for tracking droplets. The flow field, the temperature distribution, the soot and chemical species concentrations, and the trajectories of oil droplets and coke particles were numerically determined for an industrial-type oil-fired furnace operating with a single swirling burner

2 Mathematical and physical modelling

2.1 Basic transport equations and physical modelling for gas-phase

The mass, momentum, energy and chemical species Eulerian transport equations for a three-dimensional turbulent reacting flow are applied in their Cartesian co-ordinate form.The two-equation model[10], in which equations for the turbulent kinetic energy k and its dissipation rate ε are solved, appears to be satisfactory for applications of the present kind[1,11]. The combustion model was based on

the idea of a single step and fast reaction between the gaseous fuel—vaporised at the droplet surface and diffused to the flame front—and the oxidant, assumed to combine in stoichiometric proportion. It was also assumed that all species and heat diffuse at the same rate, and hence that the instantaneous gas composition can be determined as a function of a conserved scalar variable[12]. Any conserved scalar may be chosen, and here the mixture fraction f, defined as the mass of burnt and unburnt fuel present, was used.

In a turbulent flow, the mixture fraction fluctuates, and knowledge of its mean value is insufficient to allow the determination of the values of quantities such as density and temperature, because of the non-linearity of the relationships. A statistical approach to describe the temporal nature of the mixture fraction fluctuations was adopted. The time-averaged value of any property ϕ solely dependent on f can be determined from the convolution of ϕ and the probability-density function pdf. The clipped-Gaussian pdf for mixture fraction[13], which is defined completely by its mean value f and variance g, was employed. The variables f and g also obey modelled transport equations.

The discrete transfer procedure[14] for radiation predictions was utilised in this study. It is based on the solution of the fundamental radiative transfer equation within discretised solid angles. Providing the hemisphere surrounding each wall grid-node is discretised into a reasonable number of elemental solid angles, the method has proved to be accurate and, also importantly, it is applicable to arbitrary geometries. The last feature is of particular importance in the real world of geometrically intricate combustion chambers. The gas absorption coefficient was calculated from the two-grey-plus-a-clear-gas fit of Truelove[15]. The optical behaviour of the soot was accommodated by discretising the soot absorption coefficient such that it is uniform at empirically determined values within each of the bands of the mentioned model[15]. According to this work, the total emittance ε_m of the gas and soot mixture is given by:

$$\varepsilon_m = \sum_{n,n'} a_{m,n,n'}(T_g)\{1-\exp[(-k_{g,n}(p_w+p_c)-k_{s,n'}c)L]\} \quad (1)$$

where:

$$\sum_{n'} a_{m,n,n'}(T_g) = a_{g,n}(T_g) \quad (2a)$$

$$\sum_{n} a_{m,n,n'}(T_g) = a_{s,n'}(T_g) \quad (2b)$$

$$a_{m,n,n'}(T_g) = b_{1,n,n'} + b_{2,n,n'}T_g \quad (2c)$$

In these equations c is the soot concentration, $b_{1,n,n'}$, $b_{2,n,n'}$, $k_{g,n}$ and $k_{s,n'}$ are constants, tabulated in the work of Truelove[15] for different expansions of the mixture components and for oil and gas combustion. Additionally, p_w and p_c are the partial-pressure values for water vapour and carbon dioxide. In the present work the constants used are those corresponding to expansions of $n = 3$ (two grey plus one clear gases) and $n' = 2$.

In the radiation modelling, scattering of radiative energy was not considered. This has proved to be an acceptable simplification in flames where particulate (with characteristic dimensions below 1 μm) is essentially soot, and therefore contributing mainly to the flame emission and absorption processes. Larger particles, as in the case of coke cenospheres, are responsible mainly for the scattering of the radiative energy. This phenomenon may in turn influence the temperature distribution inside the furnace; its amplitude depends on the coke particles size and concentration. Because of the low level of particulate emissions measured at the furnace outlet, which is an indicator of the low levels of coke cenospheres inside the furnace, the effect of scattering is probably dominated by the soot effects of emitting and absorbing radiative energy.

2.2 Soot formation and oxidation models

As soot is formed in gas-phase reactions, an Eulerian approach was used and the transport equation for the soot mass fraction was built. The simple global model established by Khan & Greeves[16] was used for calculating the source term for the soot production rate:

$$S_f = C_f p_f \phi^n \exp\left(-\frac{E}{RT_g}\right) \quad (3)$$

where C_f and n are constants obtained from Abbas & Lockwood[17]. The fuel oil used by these authors to tune the model constants is the same as used for the present predictions. Since p_f, ϕ and T_g may be related to the mixture fraction, the mean value of the source term is computed from the convolution:

$$\overline{S_f} = \int_0^1 S_f p(f)\,df \quad (4)$$

where $p(f)$ is the pdf of the mixture fraction. Soot production is essentially zero for equivalence ratios less than the incipient sooting limit and for ϕ in excess of a value corresponding roughly to the upper flammability limit[18].

A simple model[19] for estimating the soot oxidation rate was adopted. It follows conventional turbulence concepts in presuming that the turbulence decay of the mixing rate is proportional to the magnitude of the time-mean soot mass fraction m_s, and to the time-scale of the large-scale turbulence motion ε/k. The overall soot burning rate, dependent also on the oxygen mass fraction to be included in the source term of its transport equation, is given by:

$$S_d = Am_s \rho \frac{\varepsilon}{k} \min\left(1, \frac{m_o}{m_s s_s + m_f s_f}\right) \quad (5)$$

where A is the model constant, m_o and m_f are the local mean oxygen and fuel mass fractions, and s_s and s_f are the stoichiometric soot and fuel oxygen requirements. The details of the model can be found in the work of Coelho and Carvalho[8].

2.3 Modelling the liquid phase

For the liquid-phase combustion model it was assumed that a finite number of droplet-size ranges represent the continuous size distribution of the actual spray. The

momentum and thermal-balance equations for the droplets were solved in Lagrangian fashion with a stochastic treatment for turbulent dispersion. According to Newton's Second Law, and assuming that the only forces acting on droplets are the drag force and the gravity, the trajectory of a single droplet is defined by:

$$\frac{\partial u_d}{\partial t} = \frac{1}{\tau_d}(u_g - u_d) + g_x \quad (6a)$$

$$\frac{\partial v_d}{\partial t} = \frac{1}{\tau_d}(v_g - v_d) + g_y \quad (6b)$$

$$\frac{\partial w_d}{\partial t} = \frac{1}{\tau_d}(w_g - w_d) + g_z \quad (6c)$$

where τ_d is the characteristic dynamic response time of a droplet, as defined in the work of Sharma & Crowe[20]:

$$\tau_d = \frac{24\rho_d D_d^2}{18\mu_g C_D Re_d} \quad (7)$$

In these equations the subscripts d and g stand for liquid and gas phases respectively, and C_D is the drag coefficient given by:

$$C_D = 24\ Re_d^{-0.84} \qquad 0 < Re_d \leq 80$$

$$C_D = 0.271\ Re_d^{-0.217} \qquad 80 < Re_d \leq 10^4 \quad (8)$$

$$C_D = 2.0 \qquad Re_d > 10^4$$

$$Re_d = \frac{\rho_f D_d \left|\overline{v_d} - \overline{v_g}\right|}{\mu_g} \quad (9)$$

In the present predictions the stochastic nature of the trajectories of the discontinuous phases (droplets and cenospheres) is accounted for by the use of the turbulent dispersion model of Dukowicz[21], which has been applied extensively to spray calculations. According to this work and to its extension done by Gosman & Ioannides[22], the gas velocities u_g, v_g and w_g (see Equations 6a to 6c) are taken as instantaneous values ($u_g = \bar{u}_g + u_g'$), where the mean velocity value $\bar{u}_g$ is obtained from the solution of the relevant momentum equation. The velocity fluctuations u_g' are randomly sampled from a Gaussian pdf with a standard deviation of $(2k/3)^{1/3}$, where k is the turbulent kinetic energy. The interaction time of each pair droplet/eddy is taken as the minimum value between the eddy life time and the time spent by the droplet to cross the eddy. A two-stage droplet life history was assumed for vaporisation of the oil droplet—heat up to the boiling temperature with no evaporation, followed by heat-transfer-controlled vaporisation[17]. The rate of change of droplet temperature T_d is computed from:

$$\frac{\partial T_d}{\partial t} = \frac{6K_g Nu}{\rho_d C_{p,d} D_d^2}(T_g - T_d) + \frac{3L}{C_{p,d} D_d}\frac{\partial D_d}{\partial t} \quad (10)$$

where D_d is the droplet diameter, K_g is the thermal conductivity of the gas, ρ_d and $C_{p,d}$ are the density and the specific heat of the liquid fuel, L is the heat of vaporisation of the liquid fuel and T_g is the local gas temperature. Nu, the Nusselt Number, is given by:

$$Nu = 2.0 + 0.55 Re_d^{1/2} Pr^{1/3} \quad (11)$$

where Pr is the Prandtl number. The rate of diminution of the droplet diameter is evaluated from the droplet mass balance:

$$\frac{\partial D_d}{\partial t} = \frac{4CK_g}{\rho_d C_{p,g} D_d} \ln(1 + B) \quad (12)$$

where $C_{p,g}$ is the specific heat of the gas. The transfer number B obeys to the relationship:

$$B = \frac{C_{p,g}}{L}(T_g - T_d) \quad (13)$$

and C is an empirical correction factor to account for the effect of convection on the evaporation rate[23]:

$$C = 1 + \frac{0.278(Re_d^{1/2} Pr^{1/3})}{\left(1 + \frac{1.237}{Re_d Pr^{4/3}}\right)^{1/2}} \quad (14)$$

2.4 Modelling the formation and oxidation of coke particles

Urban & Dryer[6,9,24] have extensively studied the formation of cenospheres during the combustion of heavy fuel-oil sprays. In their experiments, every droplet with an initial diameter in the range of 200-700 μm was found to form a cenosphere. Additionally, their work established that CFI (Coke Formation Index), the mass fraction of the initial fuel droplet converted to coke, was constant for any given fuel over a wide range of combustion conditions. CFI is defined as:

$$CFI = 6\frac{D_c^2 \rho_c \tau}{D_d^3 \rho_d} \quad (15)$$

where the subscripts c and d refer respectively to the coke particulate and the oil droplet. D is the outside diameter, ρ is the density and τ is the thickness of the particle shell.

These studies[6,9,24] found that CFI, which can be taken as the coke formation potential of residual fuel oils, is constant. Moreover, the product $\rho_c \tau$ was found to be constant for a given fuel oil. Therefore the ratio of particulate diameter to droplet diameter is constant over a defined range of initial droplet sizes.

On the basis of the results of the above experiments, it was assumed in this work that a cenosphere forms at the last stage of the droplet vaporisation when its diameter reaches a critical value, determined by the value of CFI. The recently formed cenosphere itself undergoes an oxidation process, with constant diameter and falling density. Note that the experiments of Urban *et al*[6,9,24] were carried out for oil droplets with initial diameter values in the range

of 200 to 700 μm. However, for reasons of energy efficiency, in most practical cases (including the case here) the initial droplet diameters of most combusting sprays are smaller than 200 μm. As regards the extension of their results to smaller diameters, Urban *et al*[6,9,24] believed that the value of CFI should remain constant and unchanged even for droplet sizes smaller than 200 μm. However, the thin cenosphere shell model would become increasingly inaccurate with the reduction of the initial droplet diameter, and a uniform-density model would be more appropriate[24]. Therefore the uniform-density model was adopted in this work.

Coke oxidation was modelled on the assumption of a surface reaction producing CO, namely that CO subsequently oxidised to CO_2 in the gas phase. The rate of oxidation is controlled by the oxygen diffusion rate to the particle surface and by the chemical reaction rate. An apparent order of ½ for the oxygen molar concentration was assumed[25], leading to:

$$\frac{\partial m_c}{\partial t} = -\frac{k_c}{2k_d}\left[-k_c + (k_c^2 + 4k_d^4 m_{O_2})^{1/2}\right] \quad (16)$$

the diffusion rate k_d being given by:

$$k_d = \frac{4m_c D_{O_2}}{D_d} \quad (17)$$

In the previous equations m_c and m_{O_2} stand for the molar mass of carbon and oxygen, and D_{O_2} is the binary mass diffusion coefficient of oxygen in the boundary layer. Moreover, the reaction rate k_c is obtained from:

$$k_c = A_c \exp\left(-\frac{E_c}{RT}\right) \quad (18)$$

where the rate constants determined by Holmes *et al*[26] were used here, and have the values A_c = 18 kg m^{-2} s^{-1} (mol m^{-3})$^{-½}$ and E_c = 78 kJ mol^{-1}. During the oxidation phase of cenospheres a constant particle diameter was assumed.

2.5 Method of solution

The control-volume approach was used in the present predictions, and it entails subdividing the calculation domain into a number of control volumes or cells. The convection terms are discretised by the hybrid central differences/upwind method. The velocities and pressures are calculated by the SIMPLE algorithm. The solution of the individual equation sets is obtained by a form of Gauss-Seidel line-by-line iteration.

3 Description of the furnace and operating conditions

The described prediction procedure was applied for the solution of the process in the three-dimensional horizontal furnace depicted in Fig.1, which is the property of ICRR[27]. Furnace dimensions are approximately 6, 20 and 5 m, respectively in the x, y and z directions, and it is equipped with a single swirling burner located in the front wall. The outlet diameter of the burner has about 18% of the equivalent diameter of the furnace cross-section. The outlet door, which is movable according to the fuel type used, is located on the left wall for oil combustion (see Fig.1). Three coaxial swirling jets were considered in the present calculations, with swirl numbers of 0.8, 0.6 and 0.4. The air is preheated to 270 °C and its flow rate is that corresponding to an excess-air value of 16%. Two non-uniform Cartesian grids comprising 40 × 44 × 45 and 60 × 66 × 67 nodes were generated for the solution of all equations, except for radiant energy. A coarser, also non-uniform, grid of 12 × 22 × 18 was selected in conformity to the finer grids for the radiation calculations.

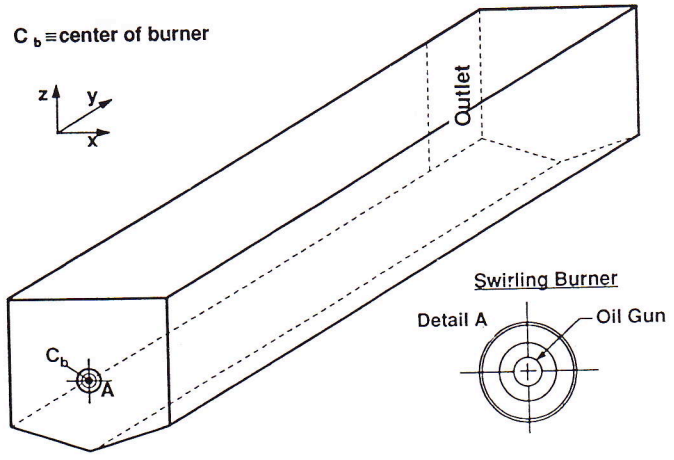

Fig.1 The ICRR furnace geometry.

Table 1 Fuel properties

	%
Carbon	85.4
Nitrogen	0.48
Hydrogen	10.8
Sulphur	2.8
Oxygen	0.5
Ash	0.02

Gross calorific value, J kg^{-1}	42.51×10^6
Latent heat, J kg^{-1}	2.73 ×10^5
Specific heat, J kg^{-1}	2.52 ×10^3
Density, kg m^{-3}	988
Viscosity (75 °C), Pa.s	0.112
Saturation temperature, °C	180

Table 2 Initial droplet sizes of the spray

Diameter, μm	Mass fraction, %
5.8 - 7.2	1.6
7.2 - 9.1	2.3
9.1 - 11.4	3.3
11.4 - 14.5	4.9
14.5 - 18.5	7.1
18.5 - 23.7	9 7
23.7 - 30.3	12.6
30.3 - 39.0	15.2
39.0 - 50.2	16.0
50.2 - 64.4	13.8
64.4 - 84.6	9.1
84.6 - 112.8	3.6
112.8 - 160.4	0.8

The properties of both the fuel oil used and the inlet spray are listed in Tables 1 and 2. By comparison of these properties with those presented by Urban *et al*[24], the CFI value was evaluated. The continuous distribution of droplet diameters of the inlet spray was discretised into 13 classes, with diameter range values based on the experiments and predictions of Carvalho *et al*[28]. The mass fraction of the droplets contained in each class are also listed in the tables. Droplets were tracked from 5 positions of the oil gun, corresponding to the grid nodes defining it. For each droplet size and initial position, and because of the stochastic nature of the procedure, 10 representative droplet trajectories were tracked in order to simulate the turbulent dispersion, and the total number of tracked trajectories were assumed to be representative of the actual spray.

For the investigation of the distribution of cenospheres inside the furnace, oil droplets, coke particles and completely burnout ash particulate trajectories were tracked in Lagrangian fashion, according to Newton's Law equations, as already mentioned. In the radiation modelling the refractory-lined walls were considered as opaque grey surfaces with an emissivity of 0.7. The application of the discrete transfer method requires the specification as boundary conditions of the wall temperatures or, alternatively, of the heat fluxes to the walls. In the present study, and because the heat fluxes values are unknown, the boundary conditions employed were prescribed temperatures.

4 Results and discussion

4.1 Standard operating conditions

4.1.1 Flow-field pattern and temperature distribution

The predicted flow-field pattern for an oil flow rate of 0.9 kg s^{-1} is shown in Fig.2, for planes normal to the three spatial directions. It can be observed that the combusting flow develops forward along the axis of the burner, and is directed to the left-hand side of the furnace near the outlet. Since the burner is small relative to the furnace dimensions, large recirculation zones are formed in the vicinity of the furnace walls in the near-burner region. These recirculation zones are strong enough to affect the flow near the front wall. Fig.2 also shows that the inlet jet is deflected slightly downwards and leftwards. The jet deflection to the bottom of the furnace is due to the pushing effect of the upper recirculation zone and to the pulling effect of the geometric design of the bottom part of the furnace. The deflection to the left is due to the location of the outlet door; as a result, the inlet swirling core moves downwards and leftwards, and eventually disappears.

Fig.3 shows the temperature distribution on vertical and horizontal planes containing the burner. A region along the burner axis exhibits high temperature values, which denotes the flame edge. The flame length is about 1/3 of the total furnace length, a value that was confirmed by visual observation of the furnace running under these operating conditions, and the highest temperature occurs in the vicinity of stoichiometry.

4.1.2 Formation, oxidation and distribution of soot

The predicted mass concentration of soot is depicted in Fig.4 in a horizontal plane containing the burner. As can be seen, soot is concentrated mainly within the flame envelope where the mixture is rich (very low oxygen concentrations) and the temperature is high. Outside the flame edge, the presence of soot is hardly detectable, as it was almost completely oxidised. Actually, most reasonably operated and maintained modern burners ensure complete oxidation of soot.

In order to confirm the high oxidation rate of soot, a fuel-rich operating condition for an equivalence ratio of 0.93 was predicted. The temperature in the flame front was found to be higher than that in the case of the furnace operating with an equivalence ratio of 1.16. The predicted soot concentrations exhibited a similar behaviour, as can be observed by comparing the results of Figs.4 and 5, but slightly higher soot concentrations were found within the flame envelope in the fuel-rich operating conditions, although with higher concentration values in the flame front, the soot formed was almost all oxidised. From these results it can be concluded that the distribution of soot depends strongly on temperature levels and oxygen concentration.

Because of its fast oxidation (a mechanism that is controlled by the turbulent mixing rate) soot is not a major species causing fouling on the furnace walls by deposition. However, the contribution of soot to the radiation heat transfer cannot be neglected (even though it is present in only trace amounts: the maximum value of soot mass concentration is equal to 0.2 $g_{soot}\ kg^{-1}{}_{mixt}$). Indeed, it has been experimentally observed in industrial flames that the amounts of soot formed in fuel-oil flames are high enough to approach the black-body limit, and therefore its presence greatly augments the radiation heat-transfer. In the present predictions this becomes obvious in comparison of the flame temperature distributions with and without soot modelling. Fig.3 shows the temperature distribution in the case of modelling soot, whereas Fig.6 shows the same results in the case of absence of soot. Observe that the presence of soot, even in small proportions as in the present case, reduces the flame temperature by about 50 K in the present study because of the greater heat transferred by radiation to the furnace walls.

4.1.3 Formation, oxidation and distribution of particulate

According to the model used herein, cenospheres are formed immediately after the droplets vaporise. Since the initial droplet sizes are small, the vaporisation time is drastically short and cenospheres are formed early. The oxidation of cenospheres depends on both local temperature and oxygen concentration. Because of the resistance imposed by their porous structure to the oxygen diffusion process, the oxidation of cenospheres takes much longer than the vaporisation of droplets. In the present study, the residence time of part of the cenospheres was not enough for complete oxidation; indeed, the numerical results indicate that 0.54% of unburnt carbon leaves the furnace. This unburnt carbon, together with the ash content of the heavy fuel oil, constitutes the undesired particulate emissions.

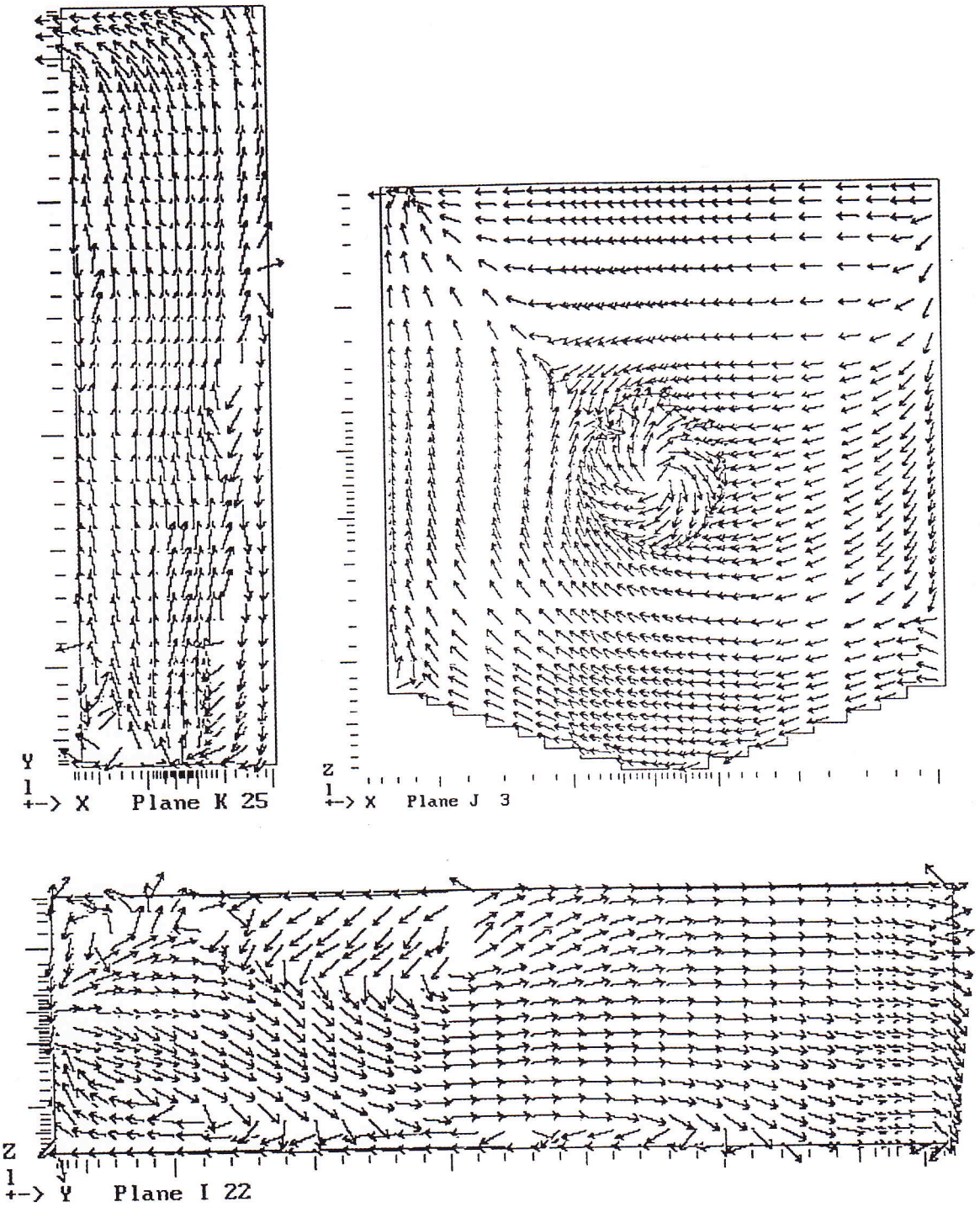

Fig.2 The flow pattern (velocity vectors are indicative of flow direction only).

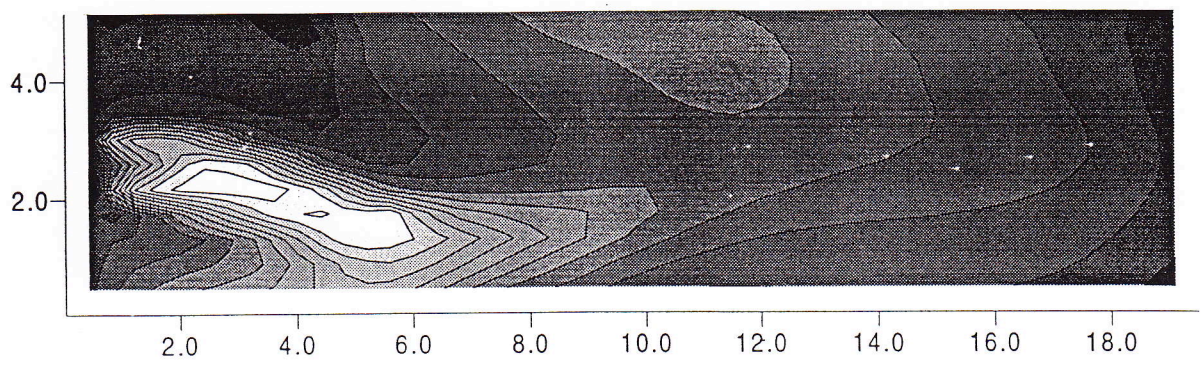

Plane I=22

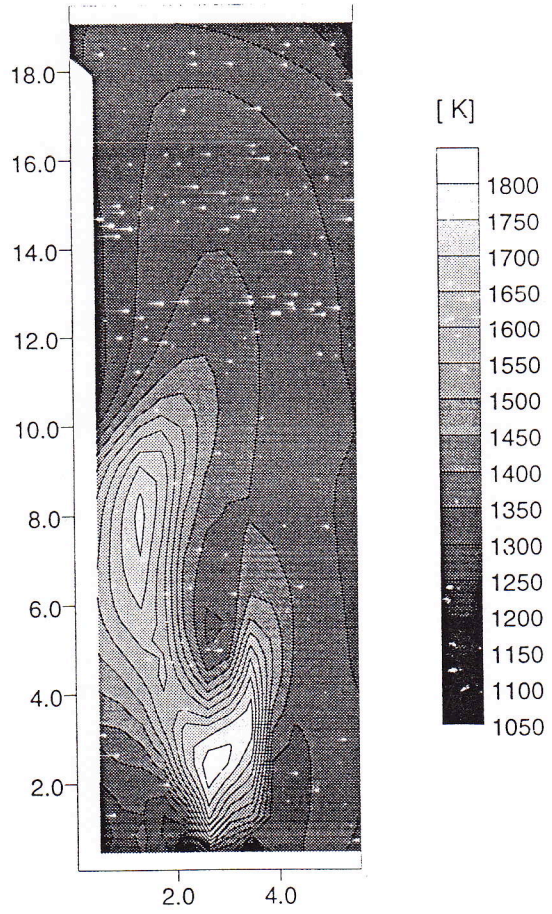

Plane K=25

Fig.3 Temperature distribution inside the furnace, taking soot into consideration.

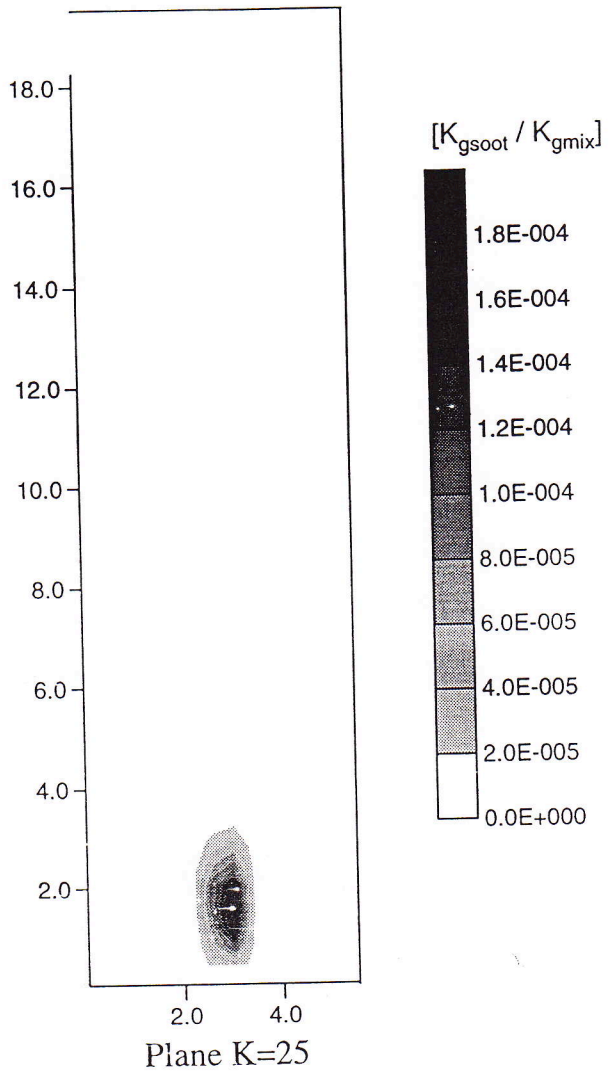

Fig.4 The soot mass concentration (kg_{soot}/kg_{mix}) in a horizontal plane containing the burner (equivalence ratio: 1.16).

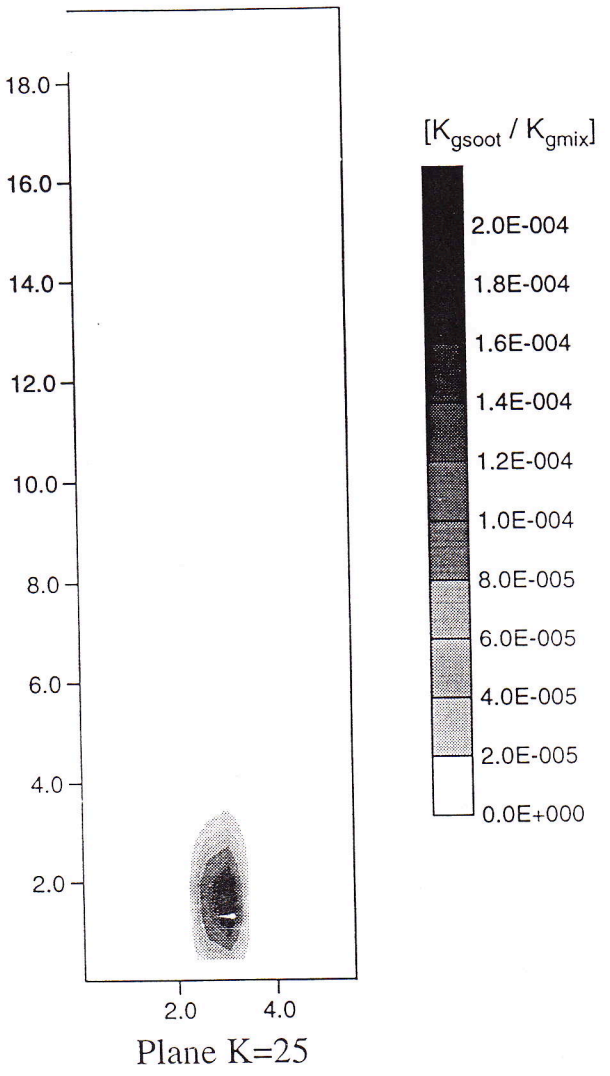

Fig.5 The soot mass concentration (kg_{soot}/kg_{mix}) in a horizontal plane containing the burner (equivalence ratio: 0.93).

Moreover, it is predicted with the present model that those particulate emissions at the furnace outlet have a concentration of 408 mg m^{-3}. In practice, the levels measured in the rig are about 0.13% of unburnt carbon leaving the furnace, and the particulate emissions at the furnace outlet exhibited a concentration of 100 mg m^{-3}. This indicates that the model may require some fine tuning of the constants.

The completely or partly oxidised coke particles, consisting of impurities contained initially in the fuel oil, have very low density values because of their porous structure. These particles may deposit on the furnace walls and cause fouling. In this work, the trajectories of these particles, with different sizes, were also tracked, and the results are depicted in Fig.7. As can be observed, the cenospheres mainly follow the main stream of the gas phase flow, and are dispersed by turbulent mechanisms. Most particles leave the furnace through the outlet (plane K 25 in Fig.7). However, some particles remain inside the furnace because of the shape of the gas-phase recirculation flow. It can be foreseen from those trajectories that there is a high probability of their deposition on the rear wall and on the left wall. This is obvious from Fig.8, where the number of particles per cubic metre is shown in the rear wall (J 44) and in the left wall (I 3).

The results allow the inference that cenospheres from oil combustion have a higher probability than soot to deposit on the furnace walls and cause fouling. Relative to gas combustion, particulate emissions are also expected to be higher.

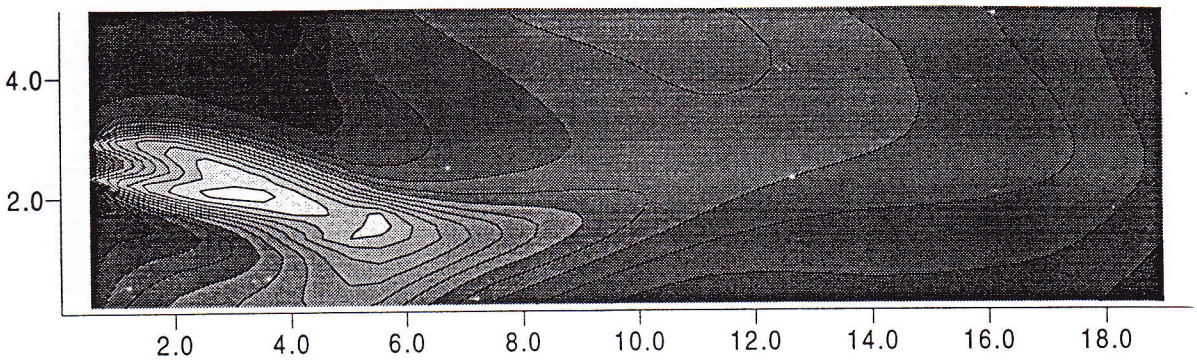

Plane I=22

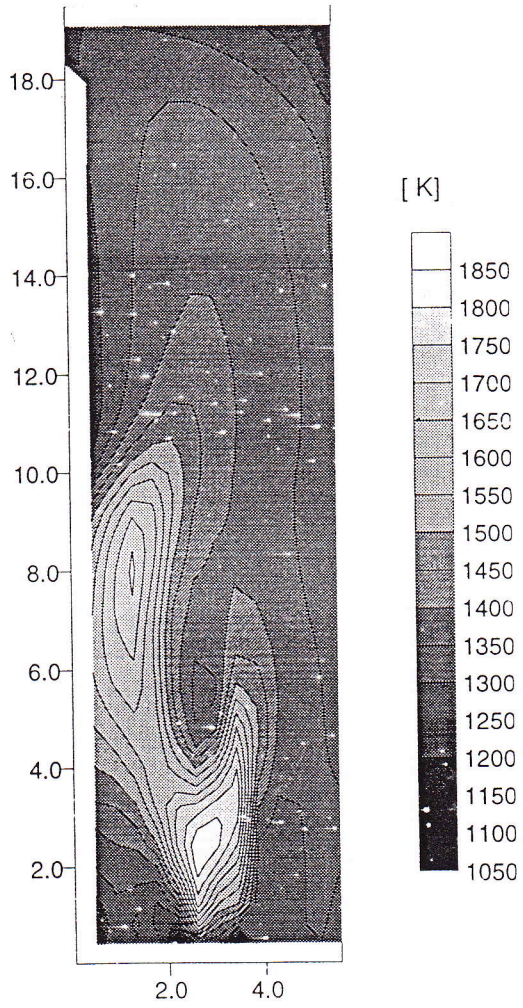

Plane K=25

Fig.6 Temperature distribution inside the furnace, not taking soot into consideration.

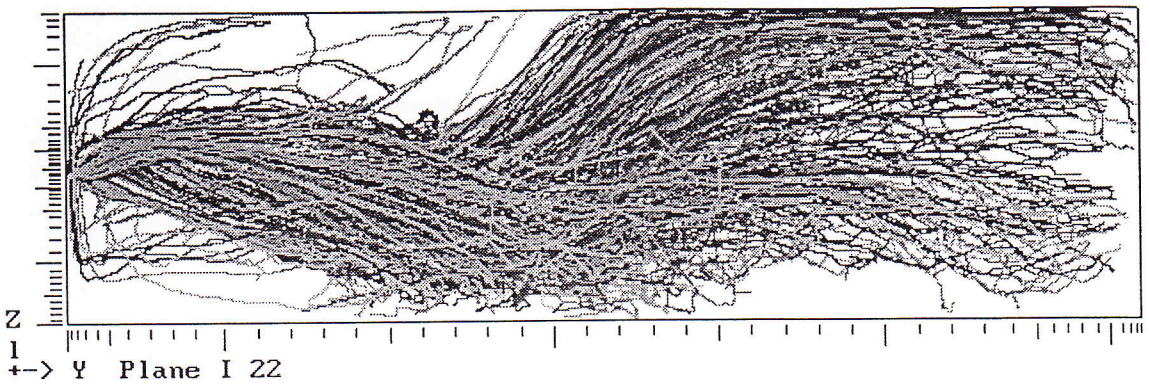

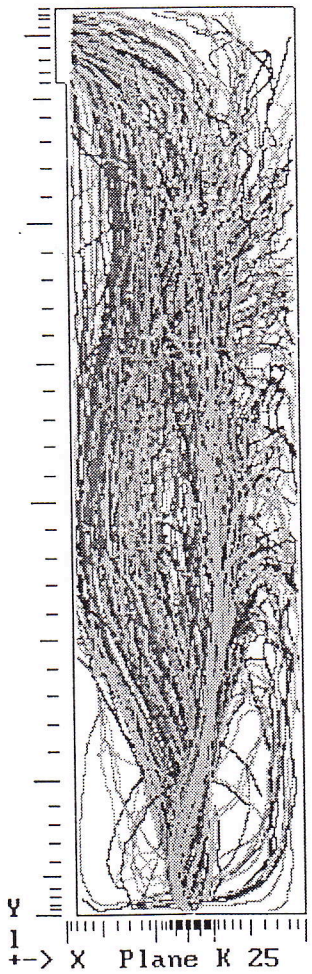

Fig.7 Trajectories of coke particles.

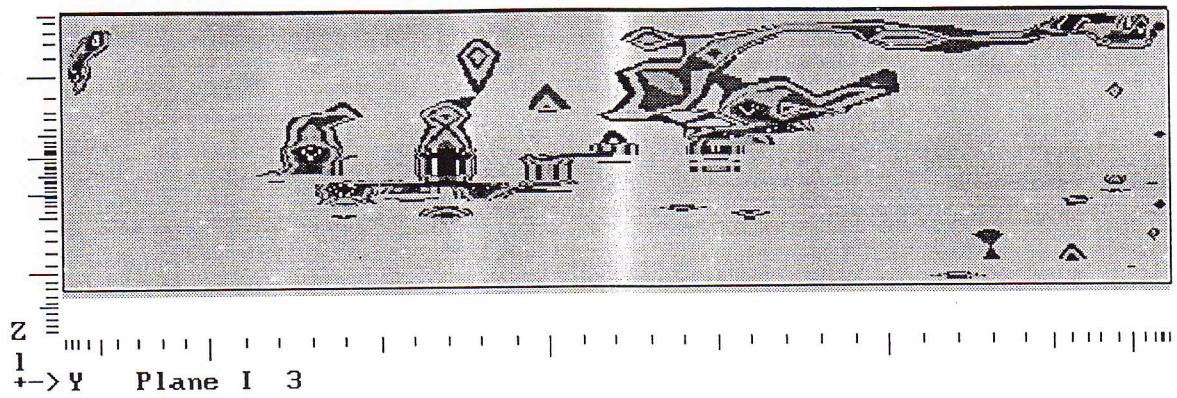

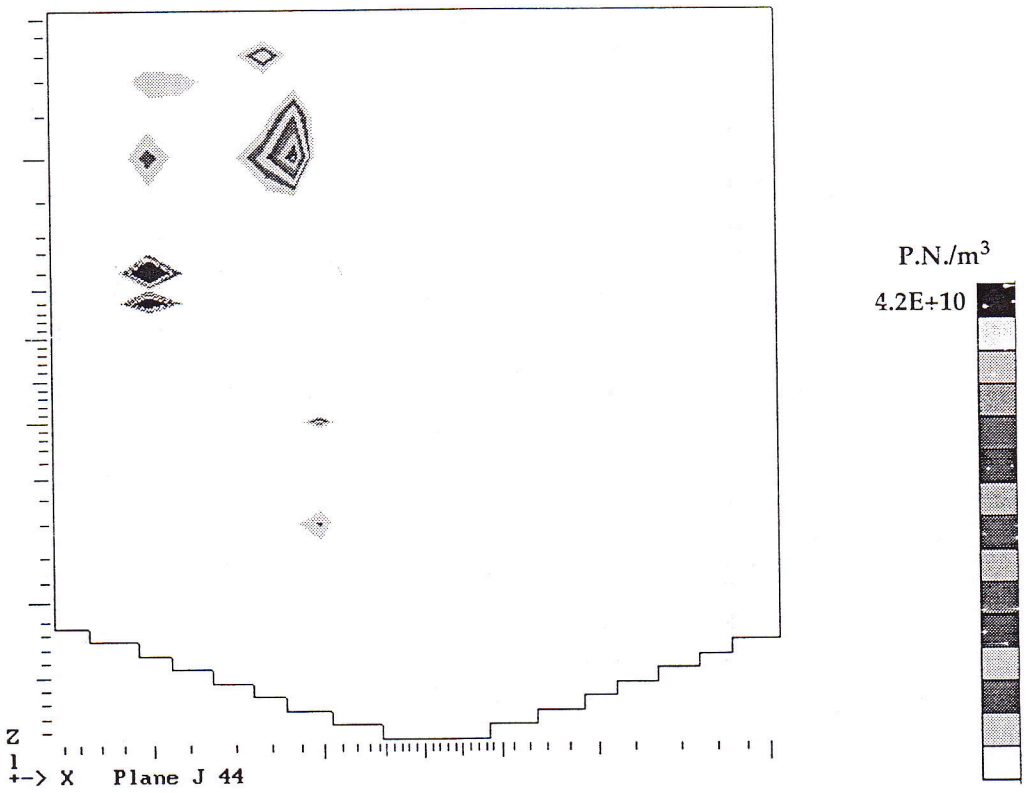

Fig.8 Particle-number concentration near the left and rear walls.

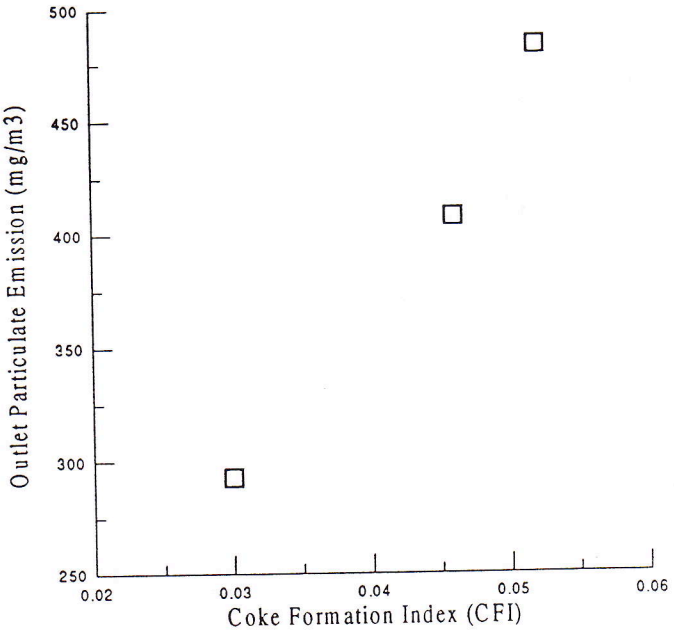

Fig.9 Effect of fuel type on particulate emissions at the furnace outlet.

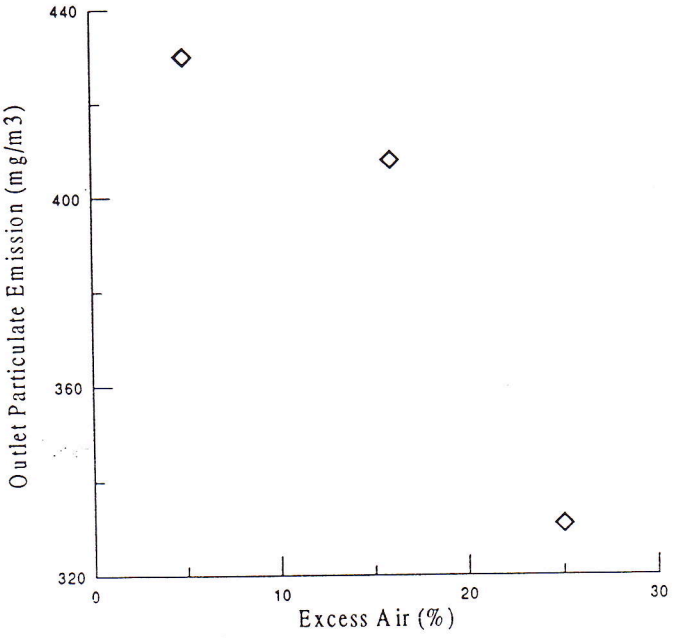

Fig.10 Effect of excess-air level on particulate emissions at the furnace outlet.

4.2 Effects of grid refinement, type of fuel oil and excess-air level

In order to study the dependence of the results with the grid refinement, two grids comprising 40 × 44 × 45 and 60 × 66 × 67 nodes were used in the present predictions. Because of its influence in all remaining calculated parameters, temperature was chosen for comparison purposes. The temperature profiles obtained with the two grids were similar (virtually coincident), except in the near-burner region, where small differences could be detected. Therefore the results obtained with the two referred grids indicate that there is only a modest degree of dependence on grid refinement, and the grid comprising 40 × 44 × 45 nodes may be considered fine enough for the objectives of the present work.

Fig.9 shows the effect of the fuel type on particulate emissions. As expected, and according to the model used herein, the critical value at which the droplet forms a cenosphere rises proportionally with the CFI value of the fuel, and cenospheres become larger and form earlier, leading to an increase of particulate emissions at the furnace outlet (see Fig.9).

Fig.10 shows the effect of excess air level on particulate emissions at the furnace outlet. The trend is well predicted; that is, the excess-air level has a major influence on the emission of particulates. In the present furnace, for excess-air levels below 25% the diminution of its level leads to a steep increase in the particulate emission. This is obviously due to the influence of oxygen concentration on the rate of carbon oxidation. In regions of oxygen deficiency there is an inhibition of carbon oxidation. Similar results were obtained by the same authors[2] in a two-dimensional study, where predictions for different excess-air values were compared with available experimental data, showing good agreement.

5 Concluding remarks

The present paper describes a two-phase flow-prediction procedure for calculating the combusting flow, heat-transfer processes and fouling trends in three-dimensional oil-fired industrial furnaces. The ability to predict the performance of fuel-oil flames poses many problems, and especially the need to model the complex mechanisms of the formation and destruction of soot and cenospheres. The particulate formed in spray combustion has been identified mainly as soot and cenospheres, and may lead to fouling, heat-transfer changes and emissions.

In the present work, a model for soot formation and oxidation was selected from the literature and was incorporated in the Eulerian framework of the global two-phase flow computational procedure. Additionally, a simple model for the formation and oxidation of cenospheres, previously developed and validated against experimental data acquired in a two-dimensional laboratory geometry, was extended and incorporated in the three-dimensional Lagrangian framework of the global procedure.

The results showed that soot is formed mainly in the gaseous fuel-rich edge of the flame, and that its formation rate depends strongly on local temperature and oxygen concentration. Moreover, its presence proved to make a major contribution to the radiative heat-transfer process against an insignificant contribution to fouling from its fast oxidation. Therefore, soot should be of concern only in terms of the optical characterisation of spray flames.

Conversely, cenospheres are formed from liquid-phase pyrolysis of vaporised droplets, and they exhibit a relatively slow oxidation rate. The completely or partly burned-out cenospheres are the major cause of fouling, and they greatly increase emissions of pollutants. Thus, the numerical characterisation of industrial oil-fired furnaces

requires the modelling of particulate formation, destruction and spatial distribution, together with their influence on furnace processes.

6 Acknowledgements

This work was performed partly with the financial support of the European Collaborative Research Programme, JOU2-CT94-0322.

7 References

1 CARVALHO M G, SEMIÃO V, LOCKWOOD F C and PAPADOPOULOS C. Predictions of nitric oxide emissions from an industrial glass-melting furnace. *J Inst Energy*, 1990, **63**, p 39.
2 YUAN J, SEMIÃO V and CARVALHO M G. Modelling and validation of the formation and oxidation of cenospheres in a confined spray flame. Accepted for publication in *Int J Energy Research*.
3 MARRONE N J, KENNEDY I M and DRYER F L. Coke formation in the combustion of isolated heavy oil droplets. *Comb Sci Tech*, 1984, **36**, p 149.
4 BOMO N, LAHAYE J, PRADO G and CLAUS G. Formation of cenospheres during pyrolysis of residual fuel oils. 20th Symp (Int) on Combustion. The Combustion Institute, 1984, p 903.
5 GLASSMAN I. Soot formation in combustion processes. 22nd Symp (Int) on Combustion. The Combustion Institute, 1988, p 295.
6 URBAN D L and DRYER F L. Heat transfer in combustion systems (ed Farouk *et al*). ASME HTD-**142**, 1990, p 83.
7 CLAYTON R M and BACK L H. Physical and chemical characteristics of cenospheres from the combustion of heavy fuel oils. *Trans ASME, J Eng Gas Turbines Power*, 1989, **111**, p 679.
8 COELHO P J and CARVALHO M G. Modeling of soot formation and oxidation in turbulent diffusion flames. *J Thermophysics Heat Transfer*, 1995, **9**, p 644.
9 URBAN D L and DRYER F L. New results of coke formation in the combustion of heavy-fuel droplets. 23rd Symp (Int) on Combustion. The Combustion Institute, 1990, p 1437.
10 LAUNDER B E and SPALDING D S. Mathematical Models of Turbulence. Academic Press, New York, 1972.
11 GOSMAN A D, LOCKWOOD F C, MEGAHED I E and SHAH N G. The prediction of the flow, reaction and heat transfer in the combustion chamber of a glass furnace. AIAA 18th Aerospace Sciences Meeting, California, 1980.
12 WILLIAMS F A and LIBBY P A. Some implications of recent theoretical studies in turbulent combustion. AIAA Paper No 80-0012, 1980.
13 LOCKWOOD F C and NAGUIB A S. The prediction of the fluctuations in the properties of free, round jet, turbulent diffusion flames. *Comb Flame*, 1975, **24**, p 109.
14 LOCKWOOD F C and SHAH N G. A new radiation solution method for incorporation in general combustion prediction procedures. 18th Symp (Int) on Combustion. The Combustion Institute, 1981, p 1405.
15 TRUELOVE J S. A mixed grey gas model for flame radiation. AERE Harwell Report No HL/76/3448/KE, 1981.
16 KHAN J H and GREEVES G. A method for calculating the formation and combustion of soot in diesel engines. Heat Transfer in Flames (ed Afgan & Beér), John Wiley & Sons, 1974, p 391.
17 ABBAS A S and LOCKWOOD F C. The prediction of several residual oil flames. *Trans ASME, J Eng Gas Turbine Power*, 1985, **107**, p 726.
18 GLASSMAN I and YACCARINO P. The temperature effect in sooting diffusion flames. 18th Symp (Int) on Combustion. The Combustion Institute, 1981, p 1175.
19 MAGNUSSEN B F and HJERTAGER B H. On mathematical modelling of turbulent combustion with special emphasis on soot formation and combustion. 16th Symp (Int) on Combustion. The Combustion Institute, 1977, p 719.
20 SHARMA M P and CROWE C T. A novel physico-computational model for quasi one dimensional gas particle flows. *Trans ASME, J Fluids Eng*, 1987, **100**, p 343.
21 DUKOWICZ J K. A particle-fluid numerical model for liquid sprays. *J Comp Physics*, 1980, **35**, p 229.
22 GOSMAN A D and IOANNIDES E. Aspects of computer simulation of liquid-fuelled combustors. *AIAA J Energy*, 1983, **7**, p 482.
23 FAETH G M. Mixing, transport and combustion in sprays. *Prog Energy Comb Sci*, 1987, **13**, p 293.
24 URBAN D L, HUEY S P C and DRYER F L. Evaluation of the coke formation potential of residual fuel oils. 24th Symp (Int) on Combustion. The Combustion Institute, 1992, p 1357.
25 SMITH I W. The combustion rate of coal chars. 19th Symp (Int) on Combustion. The Combustion Institute, 1983, p 1045.
26 HOLMES R, PURVIS M R I and STREET P J. The kinetics of combustion oil coke particles. *Comb Sci Tech*, 1990, **70**, p 135.
27 ISDALE J D. Fouling of combustion chambers and high temperature filters. 2nd periodic report of EU JOULE contract JOU2-CT94-0322, 1995.
28 CARVALHO M G, COSTA M M, LOCKWOOD F C and SEMIÃO V. The prediction of SMD and droplet size distribution for different atomisers. Proc Int Conf Mechanics Two-Phase Flows, Taiwan, 1989, p 254.

(Paper received November 1996.)